BIOCHEMISTRY
including biophysical chemistry & molecular biology

ARTICLE

pubs.acs.org/biochemistry

Mutational and Structural Studies of the PixD BLUF Output Signal That Affects Light-Regulated Interactions with PixE

Hua Yuan,[†] Vladimira Dragnea,[†] Qiong Wu,[‡] Kevin H. Gardner,[‡] and Carl E. Bauer*[,†]

[†]Department of Molecular and Cellular Biochemistry, Indiana University, Bloomington, Indiana 47405, United States

[‡]Department of Biochemistry, University of Texas Southwestern Medical Center, Dallas, Texas 75390-8816, United States

ABSTRACT: PixD (Slr1694) is a BLUF (blue-light-using FAD) photoreceptor used by the cyanobacterium *Synechocystis* sp. PCC6803 to control phototaxis toward blue light. In this study, we probe the involvement of a conserved Tyr8−Gln50−Met93 triad in promoting an output signal upon blue light excitation of the bound flavin. Analysis of acrylamide quenching of Trp91 fluorescence shows that the side chain of this residue remains partially solvent exposed in both the lit and dark states. Mutational analysis demonstrates that substitution mutations at Tyr8 and Gln50 result in the loss of the photocycle while a mutation of Met93 does not appreciably disturb the formation of the light-excited state and only minimally accelerates its decay from 5.7 to 4.5 s. However, mutations of Tyr8, Gln50, and Met93 disrupt the ability of PixD dimers to interact with PixE to form a higher-order $PixD_{10}$−$PixE_5$ complex, which is indicative of a lit conformational state. Solution nuclear magnetic resonance spectroscopy and X-ray crystallographic analyses confirm that a Tyr8 to Phe mutation is locked in a pseudo-light-excited state revealing flexible areas in PixD that likely constitute part of an output signal upon light excitation of wild-type PixD.

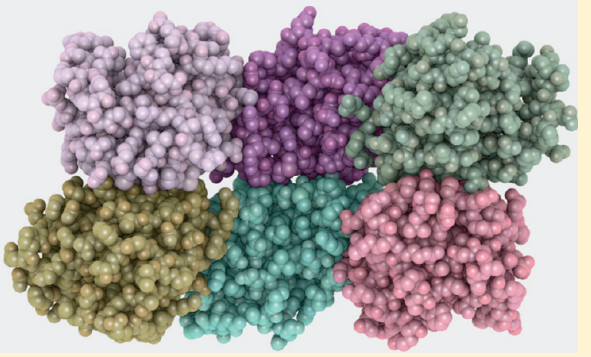

Various photosynthetic and nonphotosynthetic organisms use photoreceptors to regulate their physiology and behavior in response to light absorption at specific intensities and wavelengths. Recently, a family of photoreceptors termed blue-light-utilizing flavin (BLUF) was identified among a range of algal and bacterial proteins, all of which share a common protein fold and the use of FAD as a chromophore to absorb blue light.[1−5] Examples of well-characterized BLUF photoreceptors include AppA that controls photosynthesis gene expression in *Rhodobacter sphaeroides* in response to blue light intensity and PixD (Slr1694) that is involved in regulation of blue light phototaxis of the cyanobacterium *Synechocystis* sp. PCC6803.[1−5]

X-ray crystallographic analyses of several different BLUF domains indicate that they contain the same $\beta\alpha\beta\beta\alpha\beta\beta$ fold that is approximately 100 amino acid residues long, differing chiefly in the length of the final β5 strand and the presence of small α-helical extensions located C-terminal of the core BLUF domain.[6−10] Early attention focused on a conserved glutamine (Gln50 in PixD) proximal to FAD, of which the side chain orientation and hydrogen bond network have been topics of considerable debate.[7−16] An early model suggested that the dark-adapted BLUF domain has a Trp (Trp91 in PixD) hydrogen bonded to Gln50 and that light induces swapping of Trp91 with a nearby conserved methionine (Met93 in PixD).[6] However, recent fluorescence excitation and acrylamide quenching analysis of the BLUF domain from AppA indicated no significant light-induced movement of the homologus Trp.[17,18] These studies also suggest that Met93 rather then Trp91 is hydrogen bonded to Gln50 in the dark state as observed in 9 of 10 subunits of PixD in the crystal structure.[6]

There is considerable evidence that light excitation of the flavin ring results in alterations in the Tyr8−Gln50−Met93 hydrogen bond network. Specifically, photoexcitation of the flavin ring promotes donation of an electron and proton from Tyr8 to the light-excited flavin.[11,19] This is followed by rearrangement of a hydrogen bond between Gln50 and the flavin ring such that a new hydrogen bond is formed between Gln50 and O4 of the flavin ring.[11,19] The newly formed Gln50−O4 hydrogen bond results in a 10 nm spectral shift in flavin absorption.[20] Reversion of this spectral shift occurs upon decay to the ground state, where Gln50 is hydrogen bonded to N5 of the flavin ring. It is still debatable whether light excitation of the flavin causes a reorientation of Gln50 or a tautomeric shift that ultimately induces a change in the hydrogen bond interactions of Gln50 with the flavin ring.[16,21,22] Also not yet addressed is the question of whether Met93 remains hydrogen bonded to Gln50 when the flavin is in its light-excited state. It is also unclear how light-induced rearrangements of these protein−flavin hydrogen bonds ultimately affect the length of the β5 strand and changes in the C-terminus of the BLUF domain. Presumably, these changes are caused by a light-induced alteration of the Gln50−Met93 hydrogen bond, but this has not been directly addressed.

Prior studies have revealed that PixD exists as dimer in solution and that subsequent interaction of PixD dimers with another protein called PixE results in the formation of a large

Received: May 6, 2011
Revised: June 20, 2011
Published: June 20, 2011

oligomeric complex comprised of 10 subunits of PixD and 5 subunits of PixE.[23−25] It has been shown that light excitation of the $PixD_{10}$−$PixE_5$ supercomplex results in disassembly into PixD dimers and PixE monomers.[25] One interface among PixD dimers in the $PixD_{10}$−$PixE_5$ supercomplex involves an interaction between the α3 helix in one PixD subunit and a loop in a neighboring PixD subunit that connects strands β4 and β5. The β4 and β5 "domain interaction" loop is also known to become more dynamic when the flavin is in its light-excited state.[27,28] In this study, we address movement of the loop between strands β4 and β5 in PixD by monitoring light-driven changes in acrylamide quenching of Trp91 fluorescence in wild-type PixD as well as in Tyr8, Gln50, and Met93 mutant derivatives. We also monitor global changes in the PixD structure with a combination of solution nuclear magnetic resonance (NMR) and X-ray crystallography. Our study provides new insight into the output signal that involves an alteration of the hydrogen bond network in the Tyr8−Gln50−Met93 triad. We show that helices α1 and α3, strands β2 and β3, and loops between β4 and β5 and between α3 and α4 undergo alterations in a PixD mutant that is locked in a pseudolit state and unable to productively interact with PixE.

EXPERIMENTAL PROCEDURES

Construction of Expression Plasmids. A PixD expression plasmid for the Y8F mutant was previously constructed and provided by S. Masuda.[29] The Quick Change site-directed mutagenesis kit (Agilent Technologies) was used to construct the PixD W91A, M93A, and Q50A mutants as described previously.[6] To express PixE with a hexahistidine tag ($PixE_{His6}$) before the amino-terminal Met, its coding fragment was amplified from the genomic DNA of *Synechocystis* PCC6803 by polymerase chain reaction. The fragment was then cloned into the NdeI and SalI sites of vector pET29a (Novagen).

Protein Expression and Purification. PixD and its mutants were expressed and purified as described previously.[4] $PixE_{His6}$ was overexpressed in *Escherichia coli* Tuner (DE3) using 1 mM isopropyl β-D-thiogalactopyranoside to induce the expression at 16 °C for 16 h. The cell pellet was resuspended in lysis buffer containing 0.05 M sodium phosphate (pH 8.0), 0.3 M NaCl, 10% glycerol, and 0.02 M imidazole. The cells were then passed through a continuous flow microfluidizer (Microfluidics). After centrifugation at 20000 rpm (47810*g*) for 30 min, the supernatant was incubated with Ni^{2+}-charged His_6-tag binding resin (Novagen) at 4 °C for 1 h. The resin was then washed with 0.06 M imidazole, and the protein was eluted with 0.25 M imidazole. The $PixE_{His6}$ elution was then mixed with purified PixD (or its mutants) at a molar ratio of ∼1:2 and incubated in the dark for at least 2 h before being loaded onto a Superose 6 gel filtration column. The gel filtration analyses were performed as described previously with 10−20 μM protein in buffer containing 0.02 M Tris (pH 8.0) and 0.1 M NaCl.[25]

Acrylamide Quenching of Tryptophan Fluorescence. Fluorescence measurements were performed at 4 °C with a Perkin-Elmer LS 50B luminescence spectrometer equipped with a circulating NESLAB water bath to control sample temperature. Fluorescence quenching experiments were performed according to the method described by Eftink et al.[30] Briefly, a small aliquot of 8.0 M acrylamide, solubilized in the same buffer used for protein solution, was progressively added to 2.0 mL of protein sample. Dark and light state protein samples were obtained as described previously.[6] The fluorescence emission signal was monitored until it stabilized before the collection of each dark state data point to make sure that the protein returns to its ground state. The tryptophan fluorescence emission intensity at 360 nm (bandpass of 13 nm) was recorded with an excitation wavelength of 295 nm (bandpass of 5 nm). The protein samples were diluted to make sure the absorption at 295 nm was less than 0.1 to minimize the inner absorption effect. The inner filter effect caused by protein and acrylamide absorption at 295 nm and the dilution effect caused by addition of an acrylamide solution were corrected according to the method described by Coutinho and Prieto.[31] Both flavin and tryptophan fluorescence spectra were recorded before and after the quenching experiment to monitor possible spectral change caused by acrylamide.

Theoretical Background of Acrylamide Fluorescence Quenching. Acrylamide is an excellent tryptophan fluorescence quencher (Q) used to probe tryptophan positioning in a protein.[32] This quencher can decrease fluorescence emission from Trp by collisional (or dynamic) quenching, which involves diffusional collision of acrylamide with light-excited Trp (Trp*) that effectively quenches Trp*. A second quenching process is static quenching in which a "static" Trp*−acrylamide complex is present. Trp* quenching then happens nearly instantaneously because of the short distance.

For proteins that contain a homogeneous fluorophore, a combination of collisional and static quenching can be described by the Stern−Volmer relationship (eq 1):[33]

$$F_0/F = (1 + K_{SV}[Q])e^{V[Q]} \quad (1)$$

where F_0 and F are fluorescence intensities in the absence and presence of quencher, respectively, and K_{SV} and V are Stern−Volmer quenching constants used to describe collisional and static quenching, respectively.

For systems that exhibit only collisional quenching, eq 1 can be written as

$$F_0/F = 1 + K_{SV}[Q] \quad (2)$$

For proteins that contain heterogeneous fluorophores, the Stern−Volmer relationship can also be written as

$$\frac{F}{F_0} = \sum_{i=1}^{n} \frac{f_i}{(1 + K_{SVi}[Q])e^{V_i[Q]}} \quad (3)$$

where f_i is the maximum fractional fluorescence for fluorophore i and K_{SVi} and V_i are corresponding collisional and static quenching constants, respectively. If only collisional quenching is considered, eq 3 can be written as

$$\frac{F_0}{F_0 - F} = \frac{1}{[Q]} \times \frac{1}{\sum f_i K_{SVi}} + \frac{\sum K_{SVi}}{\sum f_i K_{SVi}} \quad (4)$$

or

$$\frac{F_0}{F} = \frac{1 + K_{Qeff}[Q]}{(1 + K_{Qeff}[Q])(1 - f_{aeff}) + f_{aeff}} \quad (5)$$

where $K_{Qeff} = \Sigma K_{SVi}$ is taken as an "effective" quenching constant and $f_{aeff} = (\Sigma f_i K_{SVi})/(\Sigma K_{SVi})$ is taken as an "effective" fractional maximum accessible fluorescence of which 100% indicates a homogeneous fluorophore conformation.[34]

Absorption Spectroscopy. Absorption spectra were recorded using an HP 8453E UV−visible spectrophotometer. Light state spectra were recorded for the same sample but with continuous illumination of white light from an MK II fiber optic

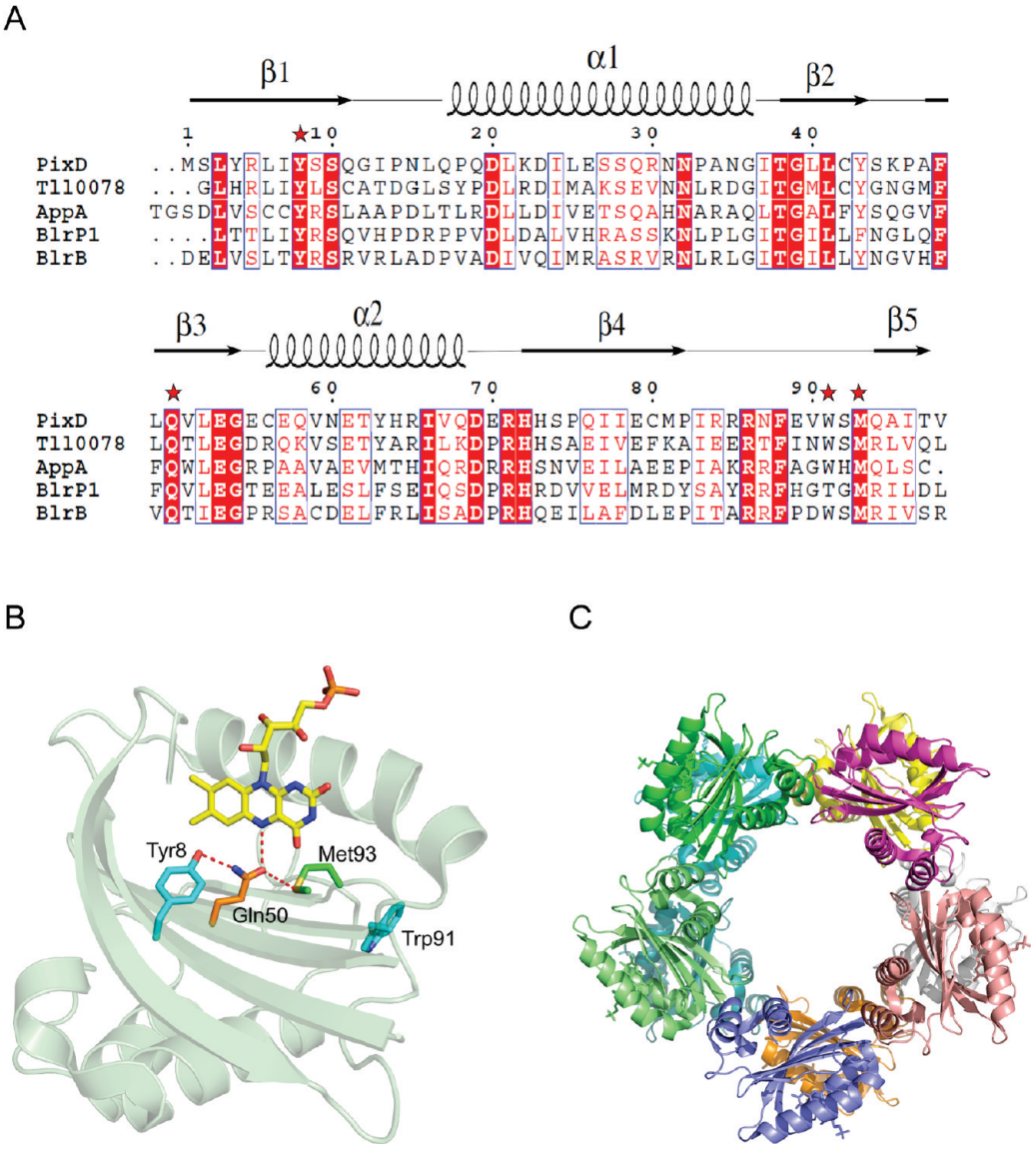

Figure 1. (A) Alignment of BLUF domains with known three-dimensional structures.[6−10,46] Conserved amino acids are shown with red backgrounds and semiconserved ones with red letters. Stars indicate residues important in BLUF domain photochemistry and are pictured in panel B. (B) PixD monomer and amino acids (and their H-bonds) critical in photochemistry. Helix α1 has been removed for the sake of clarity. (C) Wild-type PixD decamer crystal structure[6] (PDB entry 2HFN).

light source equipped with a 150 W halogen lamp at an intensity of ∼1000 μmol m^{-2} s^{-1}.

Protein Denaturation. To denature PixD, the protein was mixed with 8 M urea in 20 mM Tris (pH 8.0) and 100 mM NaCl and then incubated at room temperature for 24 h. Flavin released from denatured PixD and urea was removed by chromatographic buffer exchange in 20 mM Tris (pH 8.0) and 100 mM NaCl using a Econo-Pac desalting column from Bio-Rad.

NMR Experiments. All NMR experiments were performed at 30 °C on Varian INOVA 600 MHz and coldprobe-equipped 800 MHz spectrometers. $^{15}N-^{1}H$ TROSY experiments were conducted with uniformly ^{15}N-labeled samples with protein concentrations between 150 and 250 μM. To obtain NMR spectra of photoexcited PixD samples, we generated blue light from a 5 W Coherent Inova-90C argon laser running in single-wavelength mode at 457 nm, directing the output from this laser into a quartz fiber optic inserted into the NMR sample. Power levels at the end of this fiber were 90 mW as measured before each experiment. $^{15}N-^{1}H$ TROSY spectra of the light state of PixD were recorded by preceding each transient in the NMR experiment with a 300 ms laser pulse during the recycle delay (total recycle delay duration of ∼1.1 s).

NMRPipe[35] was used for NMR data processing and NMRViewJ[36] for data display and analysis.

Crystallization, Data Collection, and Processing. PixD-(Y8F) was crystallized using the hanging drop method against buffer containing 0.1 M $(NH_4)_2SO_4$, 0.1 M Bis-Tris (pH 6.5), 20% PEG 3350, and 0.01 M spermidine at room temperature. The crystals were transferred to crystallization buffer with 15% ethylene glycol as a cryoprotectant and then flash-frozen in liquid nitrogen. Diffraction data were collected on beamline 4.2.2 at ALS. Data were indexed and scaled using XDS.[37] The structure of Y8F was determined by molecular replacement using Phaser[38] with the wild-type PixD monomer as the search model [Protein Data Bank (PDB) entry 2HFN, chain A]. Six molecules were

dx.doi.org/10.1021/bi200701d |*Biochemistry* 2011, 50, 6365–6375

found in the asymmetric unit. After NCS averaging using ccp4 program DM had been conducted,[39] the map was good enough to allow us to adjust the model. Model building was performed in Coot.[40] The structure was refined in Phenix.refine.[41] The $P2_1$ space group was used with a twin operator of $(-h,-k,l)$ for the refinement. Pairwise root-mean-square deviation (rmsd) comparisons between all molecules of wild-type PixD (10 molecules) and the Y8F mutant (6 molecules) were performed using the McLachlan algorithm[42] as implemented in Profit (Martin, A. C. R. http://www.bioinf.org.uk/software/profit). Fits were made between the CA atoms of residues 8−140 among the wild-type ensemble and the Y8F ensemble.

RESULTS

Trp91 Remains Solvent-Exposed in Lit and Dark States, Thus Confirming a Tyr8−Gln50−Met93 Ground State. Recent mutational and spectroscopic studies of the BLUF domain of AppA demonstrated that homologues of Met93 and Trp91 do not swap positions upon light excitation (Figure 1).[18] To determine if this is also the case for PixD, we analyzed Trp fluorescence in the presence of increasing amounts of acrylamide. PixD has only a single tryptophan, Trp91, located in the loop between strands β4 and β5; thus, recording the Trp fluorescence emission intensity at 360 nm (excitation at 295 nm) in the presence (F) and absence (F_0) of acrylamide provides a measure of movement of this loop by probing for the accessibility of Trp91 to collide with this quencher. As indicated in Figure 2A, the observed F_0/F acrylamide quenching plot with wild-type denatured PixD has an upward curve that is contrasted with a downward curve observed with native folded PixD. An upward quenching plot can be assigned to static quenching, which is a process in which Trp is in contact with a quencher (acrylamide) at the time of light excitation.[30] This is contrasted by a downward curve of native folded PixD that can be attributed to collisional (or dynamic) quenching, which is a process in which light-excited Trp must subsequently collide with the quencher before excitation energy transfer occurs.

When the curve for denatured PixD is fit to eq 1, both collisional and static quenching models can be dissected to give a Stern−Volmer constant (K_{SV}) of 7.74 ± 0.16 M^{-1} and a static quenching constant (V) of 0.73 ± 0.02 M^{-1}. Note that if eq 5 is used to fit the denatured PixD quenching curve, a similar K_{SV} (7.64 ± 0.02 M^{-1}) is obtained with an f_{aeff} approaching ~100% (1.08 ± 0.01), which indicates that denatured PixD contains a homogeneous fluorophore. Inspection of the F_0/F values in Figure 2A also reveals that the quenching reaction is more efficient for denatured PixD compared to that of native PixD. This is because excitation energy transfer (quenching) is more efficient for static over collisional quenching. Illumination does not change the profile of the denatured PixD quenching curve.

In the case of native folded PixD that exhibits downward plots, only a heterogeneous fluorophore model can be fitted using eq 5, suggesting that Trp91 is in at least two states. Using eq 5 to fit a heterogeneous fluorophore for both dark- and light-adapted native PixD samples, we obtained the following: K_{Qeff} = 2.73 ± 0.20 M^{-1} and f_{aeff} = 0.69 ± 0.03 for dark adaptation and K_{Qeff} = 5.28 ± 0.18 M^{-1} and f_{aeff} = 0.76 ± 0.01 for light adaptation. For native PixD, the quenching reaction happens more efficiently in light-excited PixD relative to dark-adapted PixD as evidenced by the quenching curve of blue light-adapted protein being well above that of dark-adapted PixD (Figure 2A). This can also be concluded from values of K_{Qeff} and f_{aeff} obtained for blue

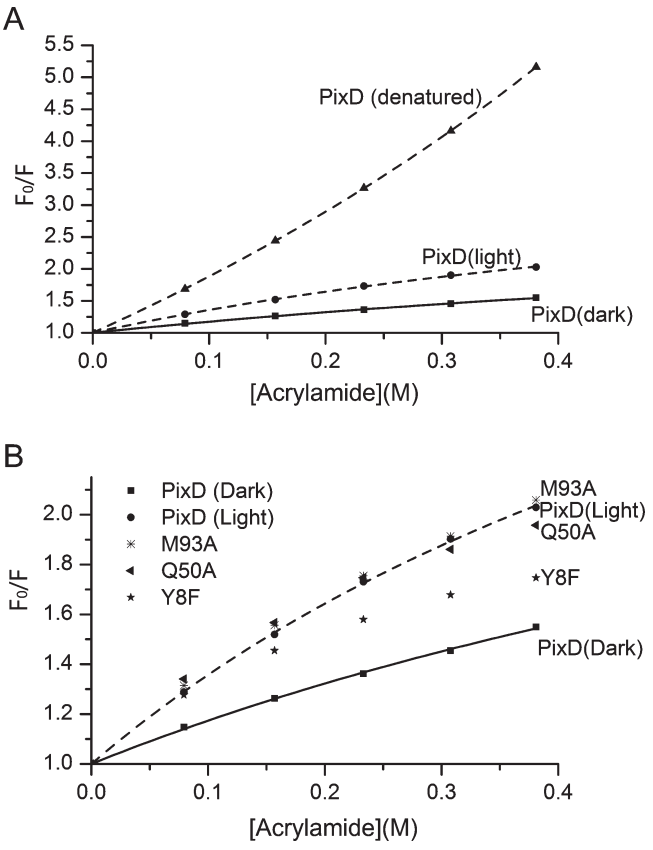

Figure 2. (A) Acrylamide quenching of tryptophan fluorescence of PixD in its native and denatured states. F_0 and F are the fluorescence intensities in the absence and presence of various concentrations of acrylamide, respectively. (B) Acrylamide quenching of tryptophan fluorescence of PixD and its mutants (Y8F, Q50A, and M93A). Only dark state data are included for the mutants because light state data are essentially the same.

light-excited PixD being larger than those of dark-adapted PixD. This result suggests that Trp91 is partially accessible to the quencher in the dark state and slightly more exposed to the quencher in the light-excited state. As in the recent acrylamide quenching study of the AppA BLUF domain,[18] these PixD quenching results do not support large movement of Trp91 into a hydrophobic pocket that contains Gln50 and FAD that should be relatively inaccessible to the quencher (inaccessible Trp104 in $AppA_{17-133}$ resulting in a horizontal quenching curve[18]). These results also suggest that the crystal structure in which 9 of 10 PixD subunits have a Tyr8−Gln50−Met93 hydrogen-bonded triad[6] represents the true dark state of this photoreceptor.

Tyr8 and Gln50 Mutants Are Spectrally Locked, while a Met93 Mutant Has a Nearly Normal Photocycle. We addressed the role of the hydrogen-bonded Tyr8−Gln50−Met93 triad by constructing substitution mutations at each of these positions. These PixD mutants were expressed, isolated, and assayed for their ability to undertake a photocycle, as well as for their ability to interact with PixE to form a $PixD_{10}$−$PixE_5$ complex. As reported previously,[4] illumination leads to a 10 nm red shift near 450 nm in the PixD visible absorbance spectrum (Figure 3A), consistent with changes to the protein−flavin hydrogen bond network. Figure 3B shows that mutating Tyr8 to Phe (Y8F) resulted in a loss of the photocycle coupled with a slight 2−3 nm blue shift of the absorption spectrum of the

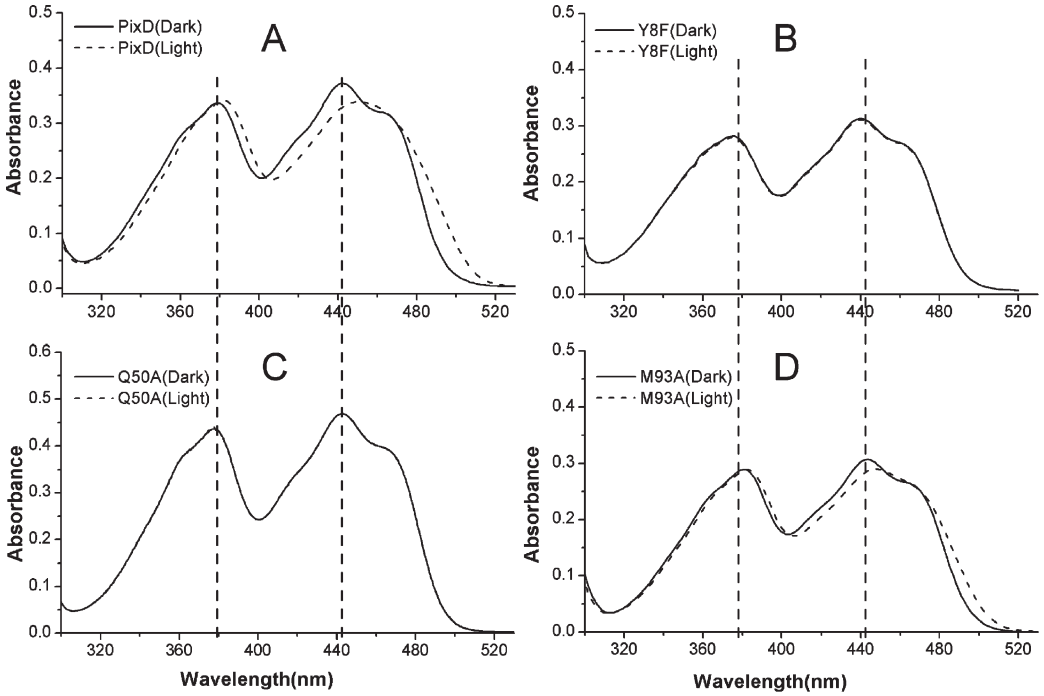

Figure 3. UV−visible absorption spectra of PixD (A) and its mutants [Y8F (B), Q50A (C), and M93A (D)] in the dark-adapted (—) and light-adapted (---) states.

flavin relative to that observed with dark-adapted wild-type PixD. A Gln50 to Ala mutation (Q50A) also disrupted the photocycle and also has a normal dark absorption spectrum with peaks at 378 and 443 nm (Figure 3C) as observed with dark-adapted wild-type PixD. These photocycle deficient mutants contrast with a Met93 to Ala (M93A) mutation at the final member of the triad that exhibits a reversible 10 nm spectral shift similar to that of wild-type PixD (Figure 3D). Analysis of the recovery rate shows that M93A exhibits a slightly faster decay to the ground state with a half-time of 4.5 ± 0.05 s relative to the half-time of 5.7 ± 0.13 s observed with wild-type PixD. In summary, Tyr8 or Gln50 mutations in the Tyr−Gln−Met triad completely eliminate the PixD photocycle, while changing Met93 has an only minimal effect on the timing of the photocycle.

Mutations in the Tyr8−Gln50−Met93 Triad Lock the Peptide into Pseudolit States. We recently demonstrated that addition of PixE promotes the assembly of PixD dimers into a $PixD_{10}$−$PixE_5$ supercomplex in the dark and that exposure to light dissociates the supercomplex back to PixE monomers and PixD dimers.[25] We can therefore utilize the ability of PixE to promote formation of a $PixD_{10}$−$PixE_5$ supercomplex as a measure of whether PixD mutants mimic a dark- or light-induced signaling state (Figure 4). For this analysis, 10−20 μM wild-type PixD or various PixD mutants were mixed with PixE at a molar ratio of ~2:1, incubated in the dark for at least 2 h, and then chromatographed through a Superose 6 gel filtration column under dark and light conditions. As shown in panels A and C of Figure 4, when wild-type PixD and PixE are preincubated together and then chromatographed in the dark, there is a distinct peak at ~370 kDa (V_e = 76 mL) representing the formation of the $PixD_{10}$−$PixE_5$ supercomplex as well as the presence of some unassembled PixD dimers and PixE monomers that coelute at ~39 kDa (V_e = 90 mL). In contrast, when the mixture of wild-type PixD and PixE is chromatographed in the light, the $PixD_{10}$−$PixE_5$ supercomplex is absent, with only a single peak eluting at ~39 kDa. This result mimics our previously published study of wild-type PixD and PixE.[25]

We next assayed the Y8F and Q50A PixD mutants for their ability to participate in forming a $PixD_{10}$−$PixE_5$ supercomplex. As shown in Figure 4B, both of these mutants were defective in associating with PixE in the dark. This result indicates that these mutants may mimic the lit state even though they exhibit dark state UV−visible absorbance spectra. This result is supported by acrylamide quenching data (Figure 2B) that indicate that these mutants also exhibit a more Trp-exposed phenotype characteristic of light-adapted PixD. Similar analysis of the PixD M93A mutant shows that this protein is also unable to form a complex with PixE (Figure 4B), suggesting that this mutant is structurally exhibiting the lit state. This is surprising as the M93A mutant exhibits a nearly normal photocycle with regard to spectral shift and length of the photocycle, suggesting that this mutation interferes with transmission of structural changes from the chromophore through the rest of the protein rather than altering the photochemical step itself. Acrylamide quenching data (Figure 2B) also indicate that this mutant constitutively exhibits a more Trp-exposed phenotype as is expected from a protein in a lit state even when assayed under dark conditions. Finally, we also undertook similar studies with the W91A mutant PixD that exhibits a normal 10 nm spectral shift and a significantly increased rate of decay to the ground state (half-time of 0.62 ± 0.04 s). The W91A mutant normally forms the $PixD_{10}$−$PixE_5$ supercomplex in the dark and dissociates out of this complex when illuminated, indicating that the W91A mutant is able to undergo a normal conformational change between dark and lit states (Figure 4B). This contrasts with the M93A mutation that also retains a photocycle but lacks formation of a normal dark state structure that is needed for interaction with PixE.

NMR and X-ray Crystallography Analyses Indicate That Y8F Is Locked in a Pseudolit State. We utilized a combination of $^{15}N-^{1}H$ TROSY NMR spectroscopy and X-ray crystallization

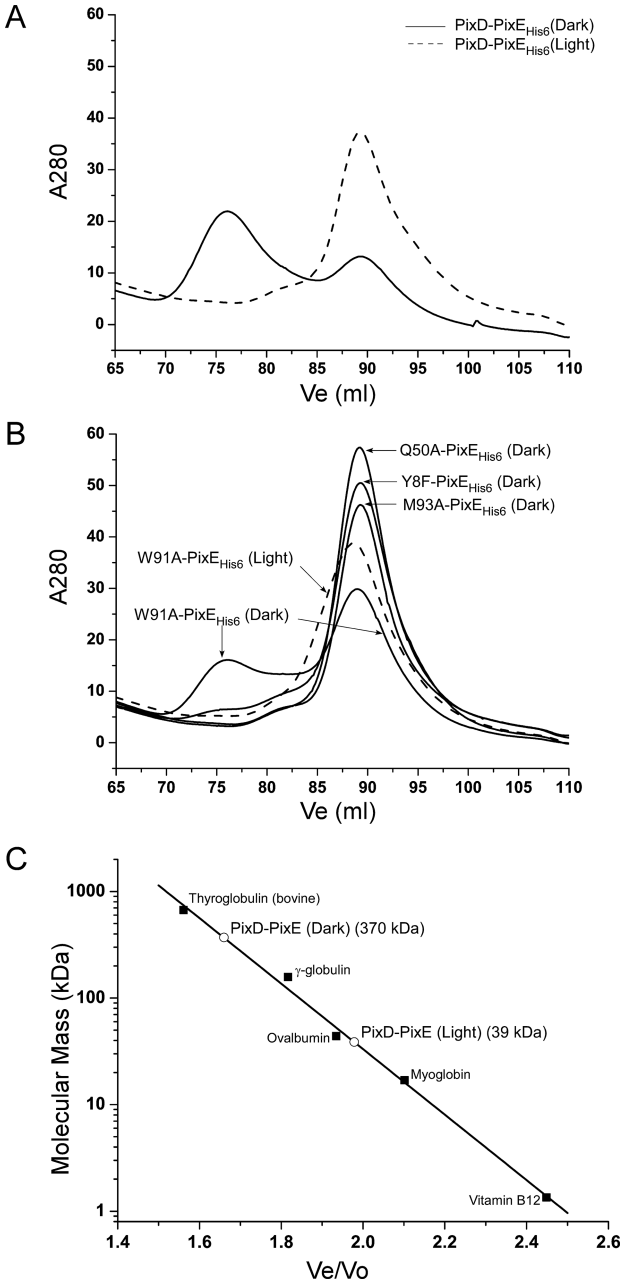

Figure 4. Gel filtration profiles of PixD mixed with PixE$_{His6}$. For Y8F, Q50A, and M93A mixed with PixE$_{His6}$, only dark state data are shown because the lit state data are essentially the same. (A) PixD−PixE$_{His6}$ mixture run under both dark and light conditions. (B) Gel filtration profile of various PixD mutant−PixE$_{His6}$ mixtures. (C) Size of the PixD−PixE complex in comparison with molecular mass standards.

analyses to probe the structure of the Y8F and M93A mutants. On the basis of differences in signal intensity for two-dimensional ^{15}N−^{1}H TROSY spectra, the NMR data are consistent with wild-type PixD existing as an oligomer larger than the Y8F mutant at the analyzed concentrations of 150−250 μM (Figure 5). Wild-type PixD exhibits numerous changes in peak intensity and location between lit and dark states, as expected from light-dependent changes in the peptide backbone as well as changes in the oligomerization state (Figure 5A). The latter is particularly evident in the increased number of peaks observed upon illumination. In contrast, analysis of spectra of dark and lit Y8F samples shows many fewer spectral changes, with no apparent light-dependent breakage of its oligomeric state, thereby confirming that this protein is photochemically inactive (Figure 5B). Comparison of the lit wild-type ^{15}N−^{1}H TROSY spectra with the dark Y8F spectra (Figure 5C) indicates that most Y8F peaks are aligned with lit wild-type peaks. There are also a few peaks in the lit wild-type spectra that are not present in the dark Y8F spectra, indicating that Y8F is in a "pseudo" lit state rather than a true wild-type lit state. We show by crystallographic analysis below that these incongruences likely represent differences in oligomerization.

Similar two-dimensional ^{15}N−^{1}H TROSY spectral analysis of the M93A mutant is quite different (Figure 5D). This spectrum yields a large number of well-resolved ^{15}N−^{1}H TROSY peaks with intensities significantly higher than those observed with wild-type and Y8F samples. This is consistent with a symmetric complex that we presume to be dimeric from gel filtration data (Figure 4). The oligomeric state does not change with light excitation, indicating that this mutant is defective in forming the larger oligomeric structures as observed in the Y8F and wild-type PixD spectra. While illumination does not cause significant chemical shift changes, we note that it instead causes a significant decrease in signal intensity for some of the peaks as previously observed for the BlrB BLUF domain, likely because of intermediate time scale exchange broadening effects.[28] These data indicate that this protein does indeed undergo a light-dependent conformational change that is likely restricted to increased motion and structural changes in the vicinity surrounding the flavin chromophore (as indicated by the wild-type visible absorbance spectral characteristics).

After many trials to crystallize all of the studied PixD mutants, the Y8F mutant was the only one providing diffraction quality crystals, and we were successful in determining its structure (refinement parameters listed in Table 1). The Y8F asymmetric unit contains only six subunits arranged in a double-stacked semicircle (Figure 6A,B), unlike the wild-type PixD that has 10 molecules arranged as a double-stacked pentameric ring observed under two different crystallization conditions (Figure 1C).

A ribbon diagram of the structure of Y8F (Figure 6A,B) shows the arrangement of six monomers in the semicircle. As observed in wild-type PixD, this arrangement involves interactions between PixD monomers across two types of dimeric interfaces. An AB dimer is designated as a pair that contains one monomer from the top and one from the bottom ring (for example, the blue and dark pink monomers in Figure 6B), while an AC dimer is designated as a pair comprised of interacting PixD in one ring (for example, blue and salmon monomers or dark pink and green monomers in Figure 6B). We assessed which dimer pair has more contact area by performing contact analysis using the Protein Interfaces, Surfaces and Assemblies (PISA) server.[43] The average area excluded in an AB dimer is 644 Å^2, while an AC dimer average excludes 493 Å^2. The Complexation Significance Score (CSS) suggested by PISA for the AB dimer is 0.47 and for the AC dimer is zero (a higher score indicates an interface necessary for complexation). Taken together, these data suggest that the AB interface will be more stable than the AC version.

Inspection of the Tyr8−Gln50−Met93 triad in the nine wild-type PixD subunits that has Trp91 exposed shows that each of these hydrogen-bonded residues is remarkably fixed compared to Trp91 that shows some variability (Figure 6C). Similar analysis of the six Y8F subunits shows that the Phe8−Gln50−Met93 triad is much more variable. Movement of Phe8 is not unexpected as this substitution would result in a loss of the hydrogen

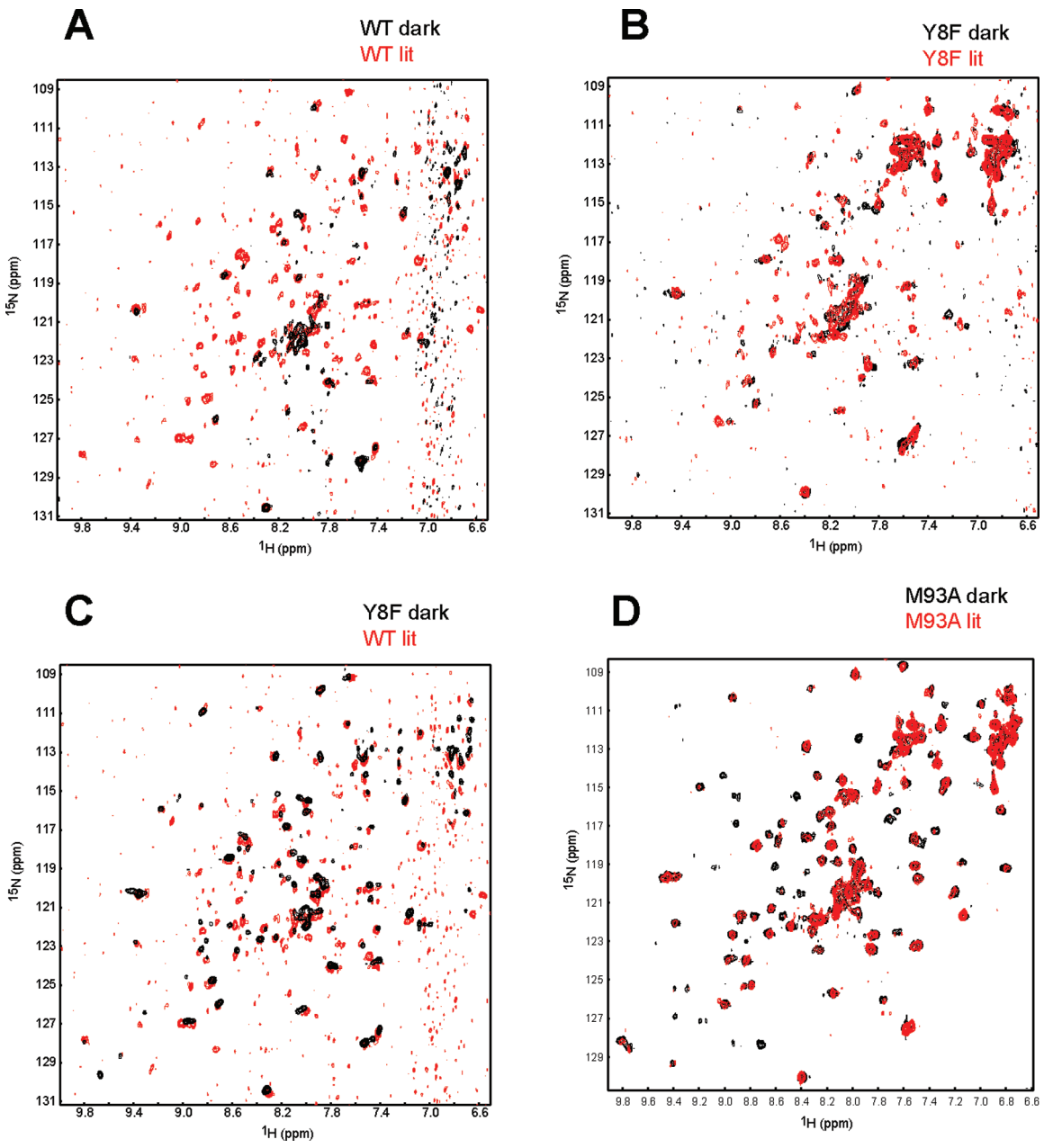

Figure 5. $^{15}N-^{1}H$ TROSY spectra of PixD under dark (black) and lit (red) conditions. Overlays are shown for wild-type (A), Y8F (B), and M93A (D) PixD proteins as indicated. (C) Comparison between wild-type lit and Y8F dark.

bond interaction that exists between Tyr8 and Gln50 in wild-type PixD. Interestingly, inspection of the distance between Met93 and Gln50 in individual Y8F subunits shows distances ranging from 2.7 to 4.4 Å (as measured between Met93 Sγ and Q50 Nε) that is contrasted by a more narrow 3.2−3.4 Å range that occurs between these residues in 9 of the 10 subunits of wild-type PixD. These distance variations, coupled with variable positions (Figure 6C), suggest that that the Phe substitution at Trp8 also likely leads the loss of a hydrogen bond between Gln50 and Met93. Another interesting observation is that Trp91 samples variable positions in the Y8F subunits with an ~180° flip to different "out" conformations. This may correspond to the increase in the level of acrylamide quenching observed with the Y8F mutant over that of dark-adapted wild-type PixD (Figure 2B).

In addition to the variability of Met93, we analyzed the variability of the backbone structure by undertaking comparative pairwise Cα rmsd analyses of wild-type PixD (10 molecules in the asymmetric unit[6]) and the Y8F mutant [six-molecule ensemble (vide infra)]. As observed in Figure 7, the rmsd values of the wild-type ensemble are generally lower than those of the Y8F ensemble. Note that the Y8F structure also has a higher overall *B* factor (91.9 Å^2 at 2.3 Å resolution) than the wild-type structure (39.4 Å^2 at 1.9 Å resolution). The larger rmsd within the Y8F ensemble and the higher *B* factor suggest that the Y8F structure presents more flexibility that is consistent with the acrylamide quenching data suggesting Y8F adopts a heterogeneous pseudolit conformation. Both wild-type and Y8F proteins exhibit similar groupings of residues with low and high rmsd values, although the

dx.doi.org/10.1021/bi200701d |*Biochemistry* 2011, 50, 6365–6375

Table 1. Summary of Crystallography Statistics (PDB entry 3MZI)

Data Collection	
space group	$P12_11$
cell dimensions	
a, *b*, *c* (Å)	41.85, 119.48, 93.26
α, *β*, *γ* (deg)	90, 102.89, 90
wavelength (Å)	1.240
resolution range (Å)[a]	49.9−2.30 (2.4−2.3)
$\langle I\rangle/\langle\sigma I\rangle$[a]	11.56 (3.13)
completeness[a]	97.3 (89.4)
R_{sym}[b]	0.081 (0.332)
redundancy	3.7
Refinement	
no. of reflections	91822
no. of unique reflections	24879
R_{work}/R_{free}	0.165/0.216
rmsd	
bond lengths (Å)	0.007
bond angles (deg)	1.241

[a] Values in parentheses are for the highest-resolution shell. [b] $R_{sym} = \Sigma(|I - \langle I\rangle|)/\Sigma I$.

Y8F backbone has additional regions with high rmsd values between residues 100 and 120 that are plotted in the Y8F structure as red and yellow in Figure 7B. The variable regions are all adjacent to each other, suggestive of concerted movements. Regions of variability are primarily localized to the C-terminal half of the BLUF domain (residues 91−130), including *β*5, α3, α4, and the loops between them. Additional variability is also observed at α1 and to a lesser extent at *β*2−*β*4. Figure 7C represents an alignment of molecule A between wild-type PixD and Y8F mutant structures. Visual inspection of both structures shows that several areas of differences in the backbone occur (designated with arrows) corresponding to regions of high flexibility as shown in the heat map in Figure 7B.

DISCUSSION

Several early studies using NMR, fluorescence, and absorption spectroscopy predicted that Trp91 (or Trp104 in AppA) was likely buried in the hydrophobic FAD binding pocket.[6,9,13,17,19,44] However, recent acrylamide quenching studies indicated that a Trp91 homologue in the native AppA is not located near the flavin in the dark state and that light excitation promoted only minimal movement of this aromatic residue.[18] Similar acrylamide quenching analysis of tryptophan in this study with PixD also indicates that Trp91 is partially solvent exposed under dark conditions with a slight increase in exposure under lit conditions. Thus, the PixD dark state also likely contains the Tyr8−Gln50−Met93 hydrogen-bonded triad that is present in 9 of 10 subunits of the PixD crystal structure where Gln50 is also hydrogen bonded to N5 of the flavin ring.[6] The observed slight increase in the level of quenching of Trp91 by acrylamide under lit conditions is consistent with the observed increase in flexibility of the *β*4 and *β*5 connecting loop that contains Trp91 upon light exposure. Comparison of Trp91 in the wild-type and Y8F crystal structures (Figure 6C) also shows that this residue seems to sample more conformations in Y8F in comparison with two main orientations in the wild-type PixD dark state. This could explain why the Y8F

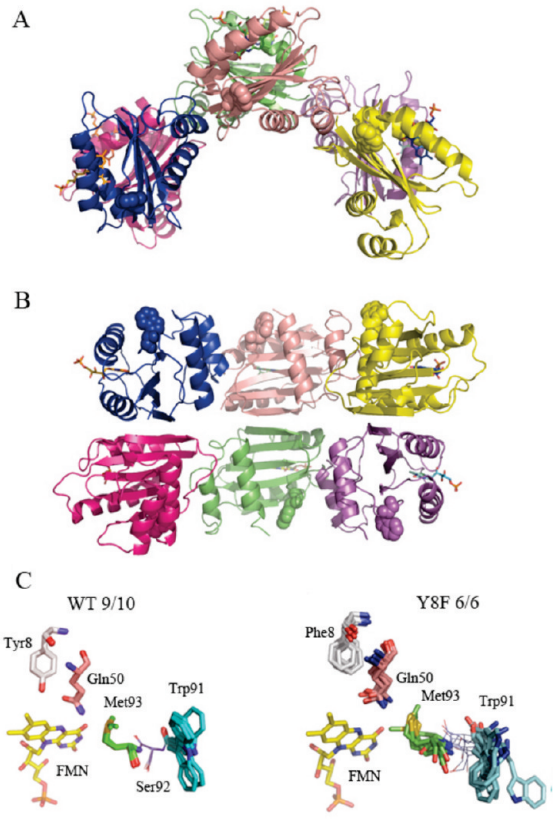

Figure 6. Crystal structure of the PixD Y8F mutant. Asymmetric unit of the Y8F crystal: (A) top view and (B) side view. Trp91 side chains are represented as spheres. (C) Superposition of Tyr8, Gln50, Trp91, and Met93 in 9 of 10 subunits of wild-type PixD and of Phe8, Gln50, Trp91, and Met93 in 6 molecules of the Y8F structure. Superposition was performed using Cα atoms of residues 5−140; only amino acids of interest are shown. The FMN molecule was not included in the alignment; however, its position in one molecule is shown for improved orientation.

acrylamide quenching curve is between the dark and lit state quenching curves of wild-type PixD. Finally, the downward curve of acrylamide quenching observed with wild-type PixD in the dark state can be explained by the presence of two main conformations of Trp91 under this condition. Dynamic sampling of different conformations by Trp91 could present a strategy for a ready response to even small perturbations of nearby hydrogen bonds (Figure 1B), either by mutation or by light-induced electron−proton transfer. Finally, mutating Trp91 itself does not affect the output signal as measured by the interaction of PixD with PixE, but it does affect the rate of the photocycle.[6] This result is consistent with the likely location of Trp91 away from the Tyr8−Gln50−Met93 hydrogen bond network. Since Trp91 is located at the start of strand *β*5 that is flexible and variable in length, a mutation in Trp91 likely influences the dynamics of this region and ultimately the return to the dark ground state.

Tyr8 is thought to initiate the BLUF photocycle through donation of an electron and proton to the light-excited flavin.[11,19] This is thought to be followed by either rotation[9,11,13] or tautomerization of Gln50,[16,21] resulting in the formation of a new hydrogen bond to O4 of the flavin that leads to a 10 nm spectral shift.[20,45] Our observation that mutations of Tyr8 and Gln50 do not exhibit a photocycle, while an Ala substitution of Met93 does lead to a productive photocycle, suggests that Met93

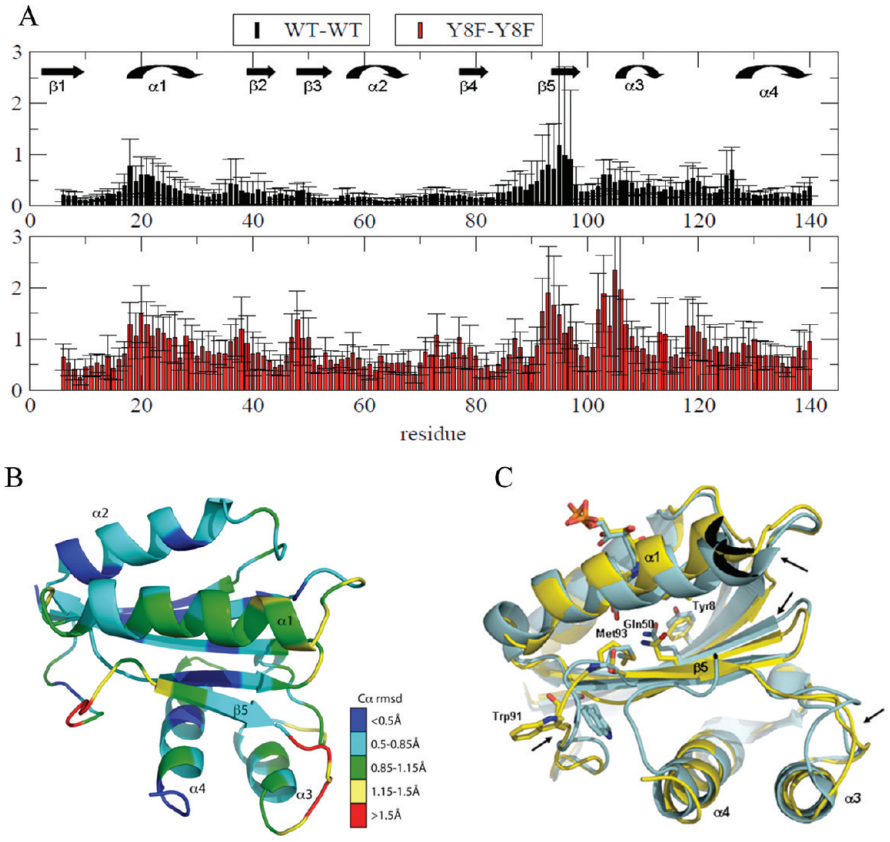

Figure 7. (A) rmsd graph for Cα atoms in an ensemble of wild-type PixD and PixD Y8F. rmsd values represent the average values with the standard deviation among the monomers. (B) rmsd values in PixD Y8F are heat-mapped to its three-dimensional structure. (C) Comparison of PixD Y8F structure (yellow) and the PixD wild-type BLUF domain (blue). Areas with the largest differences observed by visual inspection are denoted with arrows.

is not a key residue for the primary photochemistry. This is not the case for the output signal as substitution of Met93 with Ala does lead to a loss of interactions of PixD with PixE. Met93, which is conserved among BLUF proteins, must therefore be considered a key residue in propagating the output light signal. This role of Met93 is also reflected in a report that the M93A substitution in PixD does not produce a light-induced change from decamer to dimer but exists only as a dimer in solution.[26] Met93 is strategically located at a junction of the β4 and β5 loop that increases flexibility upon light excitation (Figure 7C). Presumably, light excitation of the flavin disrupts the hydrogen bond that holds Gln50 to Met93, thereby allowing this loop to become "untethered" and subsequently move. This conclusion is also supported by our Trp quenching study that shows the dark-adapted M93A mutant having an identical amount of quenching as lit wild-type PixD (Figure 2b). The loop that is "tethered" by Met93 contains Trp91, so the Met93 to Ala mutant should exhibit increased flexibility of this loop even under dark conditions, which is indeed the case. Finally, analysis of the crystal structure of the pseudolit state Y8F mutant shows that Met93 exhibits significant variability from one subunit to another in its distance from Gln50 (Figure 6C). This also suggests that Met93 is likely untethered from Gln50 in the Y8F mutant.

The asymmetry unit of the Y8F crystal contains a hexamer with subunits arranged in a double half-circle (Figure 6) instead of a decamer comprised of two complete stacked circles as observed in wild-type PixD.[6] An interesting interacting region between sets of AB dimers involves an interaction between α3 from one AB pair and the β4 and β5 flexible loop in a neighboring AB pair (Figure 8). The β4 and β5 loop contains both Trp91 and Met93 and, as discussed above, is known to undergo increased dynamic motion upon light excitation (Figure 7). Note that all these interaction faces are also present in the wild-type PixD dimer, which has a full ring comprised of five AB dimers instead of the open ring comprised of three AB dimers in Y8F. Even though one cannot rule out the possibility of crystallization conditions affecting the packing form, considering the fact that wild-type PixD adopts the same decamer conformation under two different crystallization conditions and cannot crystallize under the same conditions as Y8F, the difference in Y8F oligomerization state seen in the structure is likely biologically relevant. One significant difference in the Y8F structure is that neighboring AB dimers are somewhat tilted away from the center of the half-circle relative to neighboring pairs observed in the wild-type structure (Figure 8). Thus, if additional Y8F dimers were added to complete a circular structure, then the two ends would not align. An intriguing possibility is that this difference indicates that light illumination of wild-type PixD could disrupt the higher-order oligomer of PixD by inducing a twist to the full circle that causes disruption of the pentameric arrangement. An rmsd analysis of the Y8F structure also reveals changes in the β3 strand that contains Gln50 from where the light signal is propagated. Major changes are also present around strand β5 and helix α3 with the loop between α3 and α4 increasing flexibility. Interestingly, the loop connecting β4 to β5 in one AB dimer interacts with helix α3 of a neighboring dimer (Figure 8),

dx.doi.org/10.1021/bi200701d |*Biochemistry* 2011, 50, 6365–6375

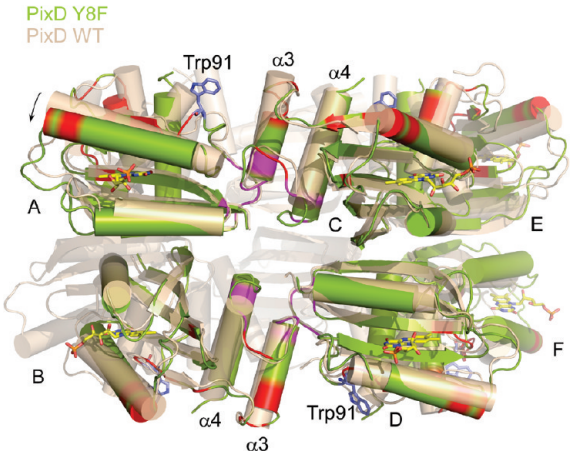

Figure 8. Superposition of Y8F structure (green) on wild-type PixD structure (wheat). Chains C and D of Y8F were superposed on Cα atoms of the wild-type structure. A tilt away from the circle center was observed on the Y8F AB dimer or EF dimer (indicated by an arrow). The interface between the AB dimer and CD dimer is highlighted in magenta. Residues with rmsd values of >1.25 among Y8F monomers are colored red. Trp91 shown as blue sticks indicates the position of the loop between strands β4 and β5.

suggesting that these regions may push against each other upon light excitation, thereby inducing a twist that disrupts the interaction between neighboring AB dimer pairs leading to disassembly of the PixD decamer.

Recently, light-excited structural changes were also reported for the BLUF domain of *Klebsiella pneumoniae* BlrP1, a light-dependent c-di-GMP hydrolase. This BLUF domain also possesses C-terminal α3 and α4 output helices akin to those observed in PixD.[27,46] Illumination led to significant changes in the position and intensity of NMR signals in residues within the β4 and β5 loop, strand β5, and the loop between helices α3 and α4.[27] When viewed in the context of the dark state crystal structure of full-length BlrP1,[46] these light-induced structural changes of the BLUF domain appear to be integral to regulating the catalytic EAL domain. We find it interesting that the changes observed in BlrP1 closely match the major changes observed in the crystal structure of the PixD Y8F mutant, suggesting that an output signal involving alteration of the flexibility of the β4 and β5 loop and its propagation through strand β5 to helices α3 and α4 may be a common output signal among BLUF domains.

Accession Codes

PDB entry 3MZI.

AUTHOR INFORMATION

Corresponding Author

*Telephone: (812)855-6595. Fax: (812) 856-4178. E-mail: bauer@indiana.edu.

Funding Sources

This study was supported by National Institutes of Health Grant GM40941 to C.E.B. and Robert A. Welch Foundation Grant I-1424 to K.H.G.

REFERENCES

(1) Gomelsky, M., and Kaplan, S. (1995) *appA*, a novel gene encoding a trans-acting factor involved in the regulation of photosynthesis gene expression in *Rhodobacter sphaeroides* 2.4.1. *J. Bacteriol. 177*, 4609–4618.

(2) Gomelsky, M., and Klug, G. (2002) BLUF: A novel FAD-binding domain involved in sensory transduction in microorganisms. *Trends Biochem. Sci. 27*, 497–500.

(3) Masuda, S., and Bauer, C. E. (2002) AppA is a blue light photoreceptor that antirepresses photosynthesis gene expression in *Rhodobacter sphaeroides*. *Cell 110*, 613–623.

(4) Masuda, S., Hasegawa, K., Ishii, A., and Ono, T. A. (2004) Light-induced structural changes in a putative blue-light receptor with a novel FAD binding fold sensor of blue-light using FAD (BLUF); Slr1694 of *Synechocystis* sp. PCC6803. *Biochemistry 43*, 5304–5313.

(5) Masuda, S., and Ono, T. A. (2004) Biochemical characterization of the major adenylyl cyclase, Cya1, in the cyanobacterium *Synechocystis* sp. PCC 6803. *FEBS Lett. 577*, 255–258.

(6) Yuan, H., Anderson, S., Masuda, S., Dragnea, V., Moffat, K., and Bauer, C. (2006) Crystal structures of the *Synechocystis* photoreceptor Slr1694 reveal distinct structural states related to signaling. *Biochemistry 45*, 12687–12694.

(7) Kita, A., Okajima, K., Morimoto, Y., Ikeuchi, M., and Miki, K. (2005) Structure of a cyanobacterial BLUF protein, Tll0078, containing a novel FAD-binding blue light sensor domain. *J. Mol. Biol. 349*, 1–9.

(8) Jung, A., Domratcheva, T., Tarutina, M., Wu, Q., Ko, W. H., Shoeman, R. L., Gomelsky, M., Gardner, K. H., and Schlichting, I. (2005) Structure of a bacterial BLUF photoreceptor: Insights into blue light-mediated signal transduction. *Proc. Natl. Acad. Sci. U.S.A. 102*, 12350–12355.

(9) Anderson, S., Dragnea, V., Masuda, S., Ybe, J., Moffat, K., and Bauer, C. (2005) Structure of a novel photoreceptor, the BLUF domain of AppA from *Rhodobacter sphaeroides*. *Biochemistry 44*, 7998–8005.

(10) Jung, A., Reinstein, J., Domratcheva, T., Shoeman, R. L., and Schlichting, I. (2006) Crystal structures of the AppA BLUF domain photoreceptor provide insights into blue light-mediated signal transduction. *J. Mol. Biol. 362*, 717–732.

(11) Gauden, M., van Stokkum, I. H., Key, J. M., Luhrs, D., van Grondelle, R., Hegemann, P., and Kennis, J. T. (2006) Hydrogen-bond switching through a radical pair mechanism in a flavin-binding photoreceptor. *Proc. Natl. Acad. Sci. U.S.A. 103*, 10895–10900.

(12) Unno, M., Masuda, S., Ono, T. A., and Yamauchi, S. (2006) Orientation of a key glutamine residue in the BLUF domain from AppA revealed by mutagenesis, spectroscopy, and quantum chemical calculations. *J. Am. Chem. Soc. 128*, 5638–5639.

(13) Grinstead, J. S., Avila-Perez, M., Hellingwerf, K. J., Boelens, R., and Kaptein, R. (2006) Light-induced flipping of a conserved glutamine sidechain and its orientation in the AppA BLUF domain. *J. Am. Chem. Soc. 128*, 15066–15067.

(14) Bonetti, C., Mathes, T., van Stokkum, I. H., Mullen, K. M., Groot, M. L., van Grondelle, R., Hegemann, P., and Kennis, J. T. (2008) Hydrogen bond switching among flavin and amino acid side chains in the BLUF photoreceptor observed by ultrafast infrared spectroscopy. *Biophys. J. 95*, 4790–4802.

(15) Iwata, T., Watanabe, A., Iseki, M., Watanabe, M., and Kandori, H. (2011) Strong donation of the hydrogen bond of tyrosine during photoactivation of the BLUF domain. *J. Phys. Chem. Lett. 2*, 1015–1019.

(16) Domratcheva, T., Grigorenko, B. L., Schlichting, I., and Nemukhin, A. V. (2008) Molecular models predict light-induced glutamine tautomerization in BLUF photoreceptors. *Biophys. J. 94*, 3872–3879.

(17) Toh, K. C., van Stokkum, I. H., Hendriks, J., Alexandre, M. T., Arents, J. C., Perez, M. A., van Grondelle, R., Hellingwerf, K. J., and Kennis, J. T. (2008) On the signaling mechanism and the absence of photoreversibility in the AppA BLUF domain. *Biophys. J. 95*, 312–321.

(18) Dragnea, V., Arunkumar, A. I., Yuan, H., Giedroc, D. P., and Bauer, C. E. (2009) Spectroscopic studies of the AppA BLUF domain from *Rhodobacter sphaeroides*: Addressing movement of tryptophan 104 in the signaling state. *Biochemistry 48*, 9969–9979.

(19) Dragnea, V., Waegele, M., Balascuta, S., Bauer, C., and Dragnea, B. (2005) Time-resolved spectroscopic studies of the AppA blue-light receptor BLUF domain from *Rhodobacter sphaeroides*. *Biochemistry 44*, 15978–15985.

(20) Masuda, S., Hasegawa, K., and Ono, T. A. (2005) Light-induced structural changes of apoprotein and chromophore in the sensor of blue light using FAD (BLUF) domain of AppA for a signaling state. *Biochemistry 44*, 1215–1224.

(21) Sadeghian, K., Bocola, M., and Schutz, M. (2008) A conclusive mechanism of the photoinduced reaction cascade in blue light using flavin photoreceptors. *J. Am. Chem. Soc. 130*, 12501–12513.

(22) Obanayama, K., Kobayashi, H., Fukushima, K., and Sakurai, M. (2008) Structures of the chromophore binding sites in BLUF domains as studied by molecular dynamics and quantum chemical calculations. *Photochem. Photobiol. 84*, 1003–1010.

(23) Okajima, K., Yoshihara, S., Fukushima, Y., Geng, X., Katayama, M., Higashi, S., Watanabe, M., Sato, S., Tabata, S., Shibata, Y., Itoh, S., and Ikeuchi, M. (2005) Biochemical and functional characterization of BLUF-type flavin-binding proteins of two species of cyanobacteria. *J. Biochem. 137*, 741–750.

(24) Kaneko, T., Sato, S., Kotani, H., Tanaka, A., Asamizu, E., Nakamura, Y., Miyajima, N., Hirosawa, M., Sugiura, M., Sasamoto, S., Kimura, T., Hosouchi, T., Matsuno, A., Muraki, A., Nakazaki, N., Naruo, K., Okumura, S., Shimpo, S., Takeuchi, C., Wada, T., Watanabe, A., Yamada, M., Yasuda, M., and Tabata, S. (1996) Sequence analysis of the genome of the unicellular cyanobacterium *Synechocystis* sp. strain PCC6803. II. Sequence determination of the entire genome and assignment of potential protein-coding regions. *DNA Res. 3*, 109–136.

(25) Yuan, H., and Bauer, C. E. (2008) PixE promotes dark oligomerization of the BLUF photoreceptor PixD. *Proc. Natl. Acad. Sci. U.S.A. 105*, 11715–11719.

(26) Tanaka, K., Nakasone, Y., Okajima, K., Ikeuchi, M., Tokutomi, S., and Terazima, M. (2011) Light-induced conformational change and transient dissociation reaction of the BLUF photoreceptor *Synechocystis* PixD (Slr1694). *J. Mol. Biol. 409*, 773–785.

(27) Wu, Q., and Gardner, K. H. (2009) Structure and insight into blue light-induced changes in the BlrP1 BLUF domain. *Biochemistry 48*, 2620–2629.

(28) Wu, Q., Ko, W. H., and Gardner, K. H. (2008) Structural requirements for key residues and auxiliary portions of a BLUF domain. *Biochemistry 47*, 10271–10280.

(29) Hasegawa, K., Masuda, S., and Ono, T. A. (2005) Spectroscopic analysis of the dark relaxation process of a photocycle in a sensor of blue light using FAD (BLUF) protein Slr1694 of the cyanobacterium *Synechocystis* sp. PCC6803. *Plant Cell Physiol. 46*, 136–146.

(30) Eftink, M. R., and Ghiron, C. A. (1976) Exposure of tryptophanyl residues in proteins: Quantitative-determination by fluorescence quenching studies. *Biochemistry 15*, 672–680.

(31) Coutinho, A., and Prieto, M. (1993) Ribonuclease T1 and alchohol dehydrogenase fluorescence quenching by acrylamide. *J. Chem. Educ. 70*, 425.

(32) Eftink, M. R., and Ghiron, C. A. (1976) Fluorescence quenching of indole and model micelle systems. *J. Phys. Chem. 80*, 486–493.

(33) Stern, O., and Volmer, M. (1919) On the quenching time of fluorescence. *Phys. Z. 20*, 183–188.

(34) Lehrer, S. S. (1971) Solute perturbation of protein fluorescence. The quenching of the tryptophyl fluorescence of model compounds and of lysozyme by iodide ion. *Biochemistry 10*, 3254–3263.

(35) Delaglio, F., Grzesiek, S., Vuister, G. W., Zhu, G., Pfeifer, J., and Bax, A. (1995) NMRPipe: A multidimensional spectral processing system based on UNIX pipes. *J. Biomol. NMR 6*, 277–293.

(36) Johnson, B. A., and Blevins, R. A. (1994) Nmr View: A Computer Program for the Visualization and Analysis of NMR Data. *J. Biomol. NMR 4*, 603–614.

(37) Kabsch, W. (1993) Automatic Processing of Rotation Diffraction Data from Crystals of Initially Unknown Symmetry and Cell Constants. *J. Appl. Crystallogr. 26*, 795–800.

(38) Mccoy, A. J., Grosse-Kunstleve, R. W., Adams, P. D., Winn, M. D., Storoni, L. C., and Read, R. J. (2007) Phaser crystallographic software. *J. Appl. Crystallogr. 40*, 658–674.

(39) Cowtan, K. (1994) *Joint CCP4 and ESF-EACBM Newsletter on Protein Crystallography*, pp 34−38.

(40) Emsley, P., and Cowtan, K. (2004) Coot: Model-building tools for molecular graphics. *Acta Crystallogr. D60*, 2126–2132.

(41) Adams, P. D., Grosse-Kunstleve, R. W., Hung, L. W., Ioerger, T. R., McCoy, A. J., Moriarty, N. W., Read, R. J., Sacchettini, J. C., Sauter, N. K., and Terwilliger, T. C. (2002) PHENIX: Building new software for automated crystallographic structure determination. *Acta Crystallogr. D58*, 1948–1954.

(42) Mclachlan, A. D. (1982) Rapid Comparison of Protein Structures. *Acta Crystallogr. A38*, 871–873.

(43) Krissinel, E., and Henrick, K. (2007) Inference of macromolecular assemblies from crystalline state. *J. Mol. Biol. 372*, 774–797.

(44) Gauden, M., Grinstead, J. S., Laan, W., Stokkum, I. H., Avila-Perez, M., Toh, K. C., Boelens, R., Kaptein, R., Grondelle, R. V., Hellingwerf, K. J., and Kennis, J. T. (2007) On the role of aromatic side chains in the photoactivation of BLUF domains. *Biochemistry 46*, 7405–7415.

(45) Masuda, S., Hasegawa, K., and Ono, T. A. (2005) Adenosine diphosphate moiety does not participate in structural changes for the signaling state in the sensor of blue-light using FAD domain of AppA. *FEBS Lett. 579*, 4329–4332.

(46) Barends, T. R., Hartmann, E., Griese, J. J., Beitlich, T., Kirienko, N. V., Ryjenkov, D. A., Reinstein, J., Shoeman, R. L., Gomelsky, M., and Schlichting, I. (2009) Structure and mechanism of a bacterial light-regulated cyclic nucleotide phosphodiesterase. *Nature 459*, 1015–1018.